Journal of The Electrochemical Society, **151** (7) A1063-A1067 (2004)
0013-4651/2004/151(7)/A1063/5/$7.00 © The Electrochemical Society, Inc.

Changes in the Lattice Constants of Thin-Film $LiCoO_2$ Cathodes at the 4.2 V Charged State

Yong Jeong Kim,[a,e] Eung-Kyu Lee,[a] Hyemin Kim,[a,e] Jaephil Cho,[b,*] Young Whan Cho,[c] Byungwoo Park,[a,*,z] Seung Mo Oh,[d] and Jong Kyu Yoon[a]

[a]*School of Materials Science and Engineering, Seoul National University, Seoul 151-742, Korea*
[b]*Department of Applied Chemistry, Kumoh National Institute of Technology, Gumi, Gyungbuk 730-701, Korea*
[c]*Nano-Materials Research Center, Korea Institute of Science and Technology, Seoul 136-791, Korea*
[d]*School of Chemical Engineering, Seoul National University, Seoul 151-744, Korea*

The lattice constants of thin-film $Li_{1-x}CoO_2$ cathodes at the 4.2 V charged states were influenced by various deposition conditions. $Li_{1-x}CoO_2$ thin films [yielding a strong (003) texture] on a Pt or Au current collector, which were unheated during sputtering deposition and *ex situ* annealed, showed negligible lattice expansion at 4.2 V during the first charge. This is in contrast to the $Li_{1-x}CoO_2$ powders exhibiting ~3% *c* axis expansion at $x \cong 0.5$ (from ~14.05 to ~14.45 Å). The total energy of the constrained $Li_{0.5}CoO_2$ lattice (0% *c* axis expansion) obtained by a pseudopotential total-energy calculation was slightly higher than that of the relaxed one by ~1.0 eV per 12 $Li_{0.5}CoO_2$ (or ~80 meV/$Li_{0.5}CoO_2$), indicating no difficulty of limited lattice expansion during the first cycle. However, splitting of the (009) diffraction peak was observed at 4.2 V as cycling proceeded: one has a lattice constant *c* of 14.01 ± 0.05 Å as $LiCoO_2$ before charging, and the other has a lattice parameter of 14.40 ± 0.05 Å, which is similar to the $Li_{0.5}CoO_2$ powders. In contrast, the lattice constants *c* of the $Li_{1-x}CoO_2$ thin films deposited at different conditions [yielding a weak (003) texture] expanded when first charged to 4.2 V, which is similar to that observed in the powder geometry.
 [DOI: 10.1149/1.1759611]

Manuscript submitted November 17, 2003; revised manuscript received January 20, 2004. Available electronically June 10, 2004.

$LiCoO_2$ is presently the most widely used cathode in rechargeable Li-ion batteries. This material has a hexagonal layered structure in which alternating planes containing Li and Co ions are separated by close-packed oxygen layers.[1-9] The $LiCoO_2$ cathode is typically charged to ~4.2 V *vs.* Li ($Li_{0.5}CoO_2$), yielding a specific capacity below ~140 mAh/g. Normally, $Li_{1-x}CoO_2$ powders expand by ~3% along the *c* axis when *x* is changed from $x = 0$-0.5.[1,2,5,6,10-14] Recent reports by Cho *et al.* on a nanoscale coating of the cathode materials with metal oxides (Al_2O_3, ZrO_2, etc.) have shown that a surface coating can suppress the lattice-constant changes in the $LiCoO_2$ powders during the first charge.[12-14] However, Chen and Dahn reported that a ZrO_2 coating on the powders has no effect on suppressing the lattice expansion.[10,11] This discrepancy may be due to the difference in the coating precursors and the uniformity of nanoscale-coating layer. Kim *et al.* recently reported that in bare $LiCoO_2$ thin films (even without metal-oxide coating), the lattice constant *c* during the first charge exhibits negligible *c*-axis expansion.[15]

In this paper, the lattice constants of thin-film $Li_{1-x}CoO_2$ cathodes at the 4.2 V charged state were investigated as a function of cycle number. The (003)-oriented $LiCoO_2$ thin films ($a \cong 2.81$ Å) on a Pt ($a/\sqrt{2} = 2.77$ Å) may be under compressive stress, while those on a Au ($a/\sqrt{2} = 2.88$ Å) may be under tensile stress. The $LiCoO_2$ thin films with a strong (003) texture show limited lattice expansion during the first cycle, unlike that observed in $LiCoO_2$ powders. In contrast, the $LiCoO_2$ thin films with a weak (003) orientation show a trend similar to the powder geometry. Pseudopotential total-energy calculation is employed to confirm the ease of negligible lattice expansion, because elastic calculation is impossible with ~3% lattice expansion.

Experimental

$LiCoO_2$ thin films were fabricated with various deposition conditions using magnetron sputtering. Approximately 500 nm thick $LiCoO_2$ thin films (1 cm^2) were deposited on a Pt or Au current collector (~200 nm) on top of the thermally oxidized SiO_2 (~150 nm)/Si(100) substrates, using a stoichiometric $LiCoO_2$ target (2 in. diam). The target was fabricated by cold-pressing commercial $LiCoO_2$ powders followed by sintering at 1000°C for 10 h in air. A TiO_2 underlayer was deposited by the reactive sputtering of Ti to improve the adhesion of current collector to the substrate. The $LiCoO_2$ targets were sputtered at a working pressure of 20 mTorr with $Ar/O_2 = 3/1$. A radio frequency (rf) power of 100 W was applied for 5 h to the target. During deposition, the substrate was either unheated or sustained at 300°C. Postdeposition crystallization of $LiCoO_2$ thin films (with unheated deposition) was obtained by 700°C annealing for 2 h in an O_2 atmosphere.

The electrochemical cells consisted of Li-metal sheets as a counter and reference electrode, a $LiCoO_2$ thin film with an approximately 1 cm^2 active area as the working electrode, and 1 M $LiPF_6$ in ethylene carbonate/diethyl carbonate (EC/DEC, 50/50 vol %, Cheil Industries, Inc.) as the electrolyte. The cells were electrochemically cycled over the voltage range 4.4-2.75 V with a specific current of 400 μA/cm^2. The cells were charged at 10 μA/cm^2 to 4.2 V during the first cycle, after five and ten cycles, and then potentiostated for 24 h so that the cells would be stabilized near 4.2 V. To characterize the $Li_{1-x}CoO_2$ thin films at the 4.2 V charged state using X-ray diffraction (XRD), the cells were disassembled in a glove box, followed by rinsing them with DEC to remove the $LiPF_6$ salt from the cathode films.

To confirm the ease of negligible lattice expansion in $Li_{1-x}CoO_2$ cathode during the first charge, the energy difference between the relaxed and constrained $Li_{1-x}CoO_2$ lattice (0% *c* axis expansion) was obtained using a pseudopotential total-energy calculation. Electronic-structure techniques enable an accurate calculation of the relative atomic-structure stability for the charged state of $Li_{1-x}CoO_2$ cathodes.[16-20] In this work, the Gibbs free energy (ΔG) was approximated to the internal energy (ΔE), because the term $P\Delta V - T\Delta S$ at room temperature was expected to be very small (<30 meV).[21] To calculate the internal energy of each configuration, this study employed the periodic boundary conditions within the gradient-corrected density-functional theory, employing the VASP code.[22,23] This method solves the Kohn-Sham equations to obtain a self-consistent valence-shell electron density within the nonlocal field of ultrasoft pseudopotential representation of the nuclei and the

* Electrochemical Society Active Member.
e Present address: L G Chemical Ltd., Taejon 305-380, Korea.
z E-mail: byungwoo@snu.ac.kr

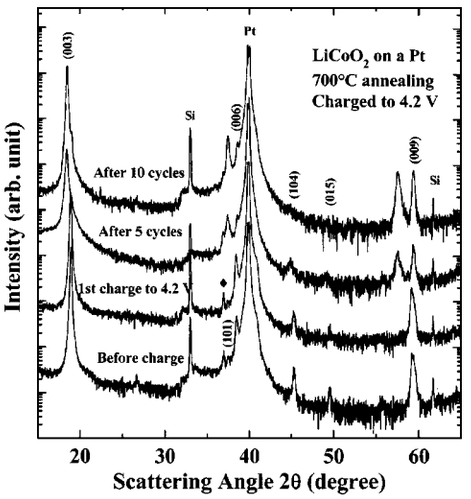

Figure 1. XRD patterns of $Li_{1-x}CoO_2$ thin films on Pt (compressive stress), before charge, after the 1st charge to 4.2 V, and after five and ten cycles (between 4.4 and 2.75 V), then charged to 4.2 V. These cathode films were unheated during sputter deposition, and *ex situ* annealed at 700°C in O_2 atmosphere. (♦) Small peak at $2\theta = 36.9°$ due to the formation of Co_3O_4.

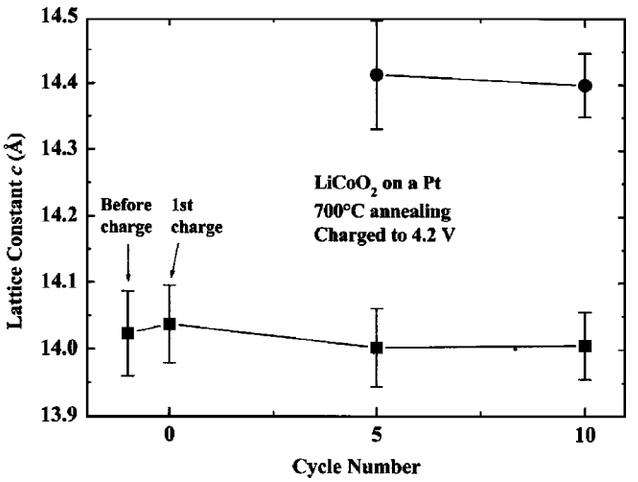

Figure 2. Changes in the lattice constant *c* as a function of cycle number for $Li_{1-x}CoO_2$ thin films on a Pt current collector when charged to 4.2 V. The lattice constant *c* was obtained from the XRD patterns shown in Fig. 1. (●) shows relaxed lattice constants of $Li_{0.5}CoO_2$, whereas the (■) lattice constants remain unchanged.

core electrons.[24-26] The calculations used a plane-wave basis with a kinetic energy cutoff of 500 eV. The *k*-point coordinates were generated using a $4 \times 4 \times 4$ Monkhorst-Pack scheme.[27] All the calculations involved a full geometry optimization. Four supercells of $x = 0$, 1/6, 1/3, and 1/2 in $Li_{1-x}CoO_2$ were examined.

Results and Discussion

Figure 1 shows the XRD patterns of the $Li_{1-x}CoO_2$ thin films on a Pt current collector, which were unheated during sputter deposition and *ex situ* annealed at 700°C in O_2 atmosphere. A single phase was obtained in the cathode film prior to charging, with the hexagonal Miller indexes (*hkl*). The XRD patterns in Fig. 1 show a strong (003) texture. The lattice constant *c* of $LiCoO_2$ thin film prior to charging is $c = 14.02 \pm 0.06$ Å, which is in good agreement with the literature data of $LiCoO_2$ powders and thin films.[1-5,10-15,28-32]

The evolution of the XRD patterns is shown in Fig. 1, when the $Li_{1-x}CoO_2$ thin films on a Pt current collector were charged to 4.2 V. After the first charge to 4.2 V, the XRD pattern shows negligible *c*-axis expansion. This is in contrast to the $Li_{1-x}CoO_2$ powders, exhibiting ~3% *c*-axis expansion at $x \cong 0.5$ (from ~14.05 to ~14.45 Å). However, splitting of the (009) diffraction peak occurs after five cycles at the 4.2 V charged state, as shown in Fig. 1. This phenomenon is more obvious at 4.2 V after ten cycles, indicating the coexistence of two distinct structures. As can be seen in Fig. 2, one has a lattice parameter $c = 14.01 \pm 0.05$ Å (same as before charging), and the other shows $c = 14.40 \pm 0.05$ Å (same as the $Li_{0.5}CoO_2$ powder value). In addition, the former (~14.0 Å) gets converted to the latter (~14.4 Å) as the cycle number increases.

$LiCoO_2$ thin films were also deposited on a Au current collector to investigate the possible stress effect on the lattice-constant changes. The lattice constant *a* of $LiCoO_2$ (~2.81 Å) is similar to the atomic distance of Pt(111) (~2.77 Å) and Au(111) (~2.88 Å). The (003)-oriented $LiCoO_2$ thin films on a Pt may be under compressive stress, while those on Au may be under tensile stress. Figure 3 shows the evolution of the XRD patterns when the $Li_{1-x}CoO_2$ thin films [yielding a strong (003) texture] on Au (unheated during deposition and *ex situ* annealing at 700°C) were charged to 4.2 V. Figure 4 presents the changes in the lattice constants *c* for the $Li_{1-x}CoO_2$ films at the 4.2 V charged state on Au as a function of cycle number (Fig. 3). When first charged to 4.2 V, the changes in the XRD patterns are not significant, with negligible lattice expansion, which is similar to the $LiCoO_2$ thin films on Pt (Fig. 1). The diffraction-peak splitting at the 4.2 V charged state is also clearly observed after five and ten cycles.

The $Li_{1-x}CoO_2$ thin films at 4.2 V have limited *c*-axis expansion during the first charge and distinct diffraction-peak splitting after cycling, regardless of the current collector. The diffraction-peak splitting occurring at 4.2 V might be because the $Li_{1-x}CoO_2$ thin films consist of restricted and unrestricted grains. Some grains exhibit limited lattice changes because of the restriction by the en-

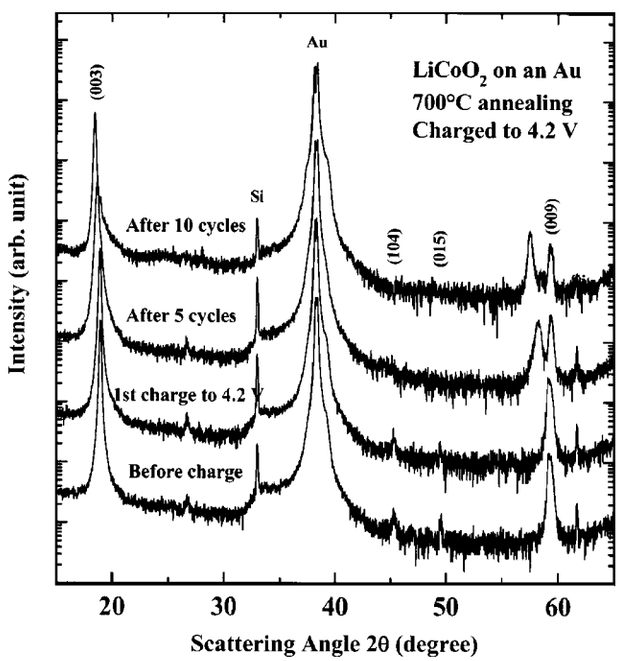

Figure 3. XRD patterns of the $Li_{1-x}CoO_2$ thin films on Au (tensile stress), before charge, after the 1st charge to 4.2 V, and after five and ten cycles (between 4.4 and 2.75 V), then charged to 4.2 V. These cathode films were unheated during sputter deposition, and *ex situ* annealed at 700°C in O_2 atmosphere.

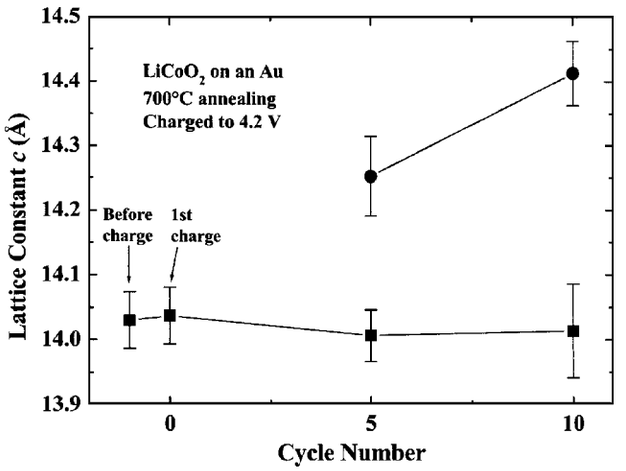

Figure 4. Changes in the lattice constant *c* as a function of cycle number for $Li_{1-x}CoO_2$ thin films on a Au current collector when charged to 4.2 V. Lattice constant *c* was obtained from the XRD patterns shown in Fig. 3.

tangled grains, while the lattice constants *c* of the unrestricted grains increase to 14.41 ± 0.05 Å when charged to 4.2 V. The lattice-constant changes from the 5th to the 10th cycle in Fig. 2 and 4 have large error bars. However, the lattice-constant expansions after ten cycles are similar each other, approaching the $Li_{0.5}CoO_2$ power value (~14.45 Å).

To confirm the ease of negligible lattice expansion in $LiCoO_2$ at 4.2 V charged state, the energy difference between $Li_{1-x}CoO_2$ with the relaxed and constrained lattice (0% *c*-axis expansion) was estimated using a pseudopotential total-energy calculation. The electronic-structure calculations were undertaken on a series of $Li_{1-x}CoO_2$ compositions, where $x = 0$, 1/6, 1/3, and 1/2. To determine the lattice parameter of the optimized $LiCoO_2$ lattice, the total energies of four primitive unit cells at Li-ordered (most stable) state were computed in the range of $c = 12.50$-15.25 Å (Fig. 5a). The computed lattice parameter of $LiCoO_2$ with the lowest energy state is $a \cong 2.84$ Å and $c \cong 13.80$ Å, which is similar to that reported by Ceder *et al.*[16,17] The difference between the calculated lattice parameter *c* (~13.80 Å) and the experimental result (~14.05 Å) of $LiCoO_2$ is within 2% (Fig. 5a). Figure 5b shows the calculated lattice parameter and the total energies of the $Li_{0.5}CoO_2$ lattice. The lattice parameter of $Li_{0.5}CoO_2$ with a minimum energy is $a \cong 2.83$ and $c \cong 14.21$ Å. As can be seen in Fig. 5, the $Li_{1-x}CoO_2$ expands by ~3% along the *c* axis when *x* changes from $x = 0$ to 0.5. Figure 6 shows the total energies of both the relaxed and constrained $Li_{1-x}CoO_2$ lattice (at Li-ordered stabel and Li-disordered metastable state, respectively). The total energy of the constrained $Li_{0.5}CoO_2$ lattice is slightly higher than that of the relaxed one by ~1.0 eV per 12 $Li_{0.5}CoO_2$ (or ~ 80 meV/$Li_{0.5}CoO_2$), which confirms the ease of limited lattice expansion during the first charge.

Figure 7a and b shows the charge-discharge profiles of $LiCoO_2$ thin films on a Pt and Au, respectively. The $LiCoO_2$ thin films were charged to 4.2 V with a current rate of 10 μA/cm^2 during the first charge, and after five and ten cycles (in the range of 4.4 and 2.75 V at 400 μA/cm^2), then potentiostated for 24 h so that the cells could stabilize near 4.2 V. The plateau at ~3.9 V corresponds to a first-order phase transition between the two hexagonal phases, and two additional plateaus above 4 V are associated with the order-disorder transitions at around $Li_{0.5}CoO_2$.[1,2,7,8] As seen in Fig. 7 (with Fig. 2 and 4), the current collector does not significantly affect the cyclability of the thin-film $LiCoO_2$ cathodes, and the profiles of $LiCoO_2$ thin films become steeper as the cycling proceeds due to the degradation of $LiCoO_2$.

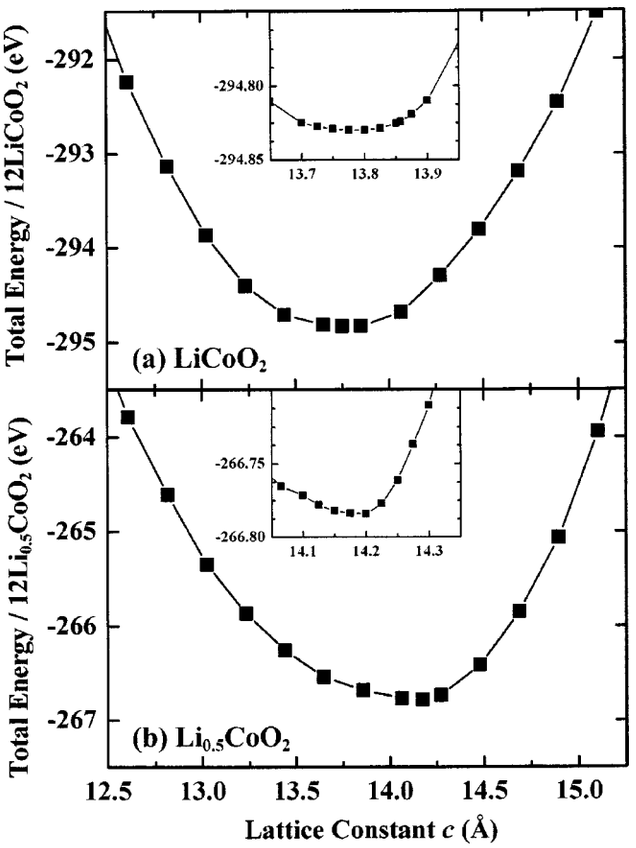

Figure 5. Total energies of (a) $LiCoO_2$ and (b) $Li_{0.5}CoO_2$ with four primitive unit cells *vs.* the lattice parameter *c*, as calculated using the pseudopotential method at Li-ordered (most stable) state.

Figure 8 shows the XRD patterns for the $Li_{1-x}CoO_2$ thin films deposited at 300°C on a Pt, without further annealing. The (003) peak prior to charging is broader than that shown in Fig. 1, and these films have the (101) orientation besides the (003) texture. The lattice constants before charging are $a = 2.82 \pm 0.01$ Å and $c = 14.13 \pm 0.01$ Å. The $LiCoO_2$ thin films deposited at 300°C have slightly larger lattice constant *c* than those deposited on unheated substrates

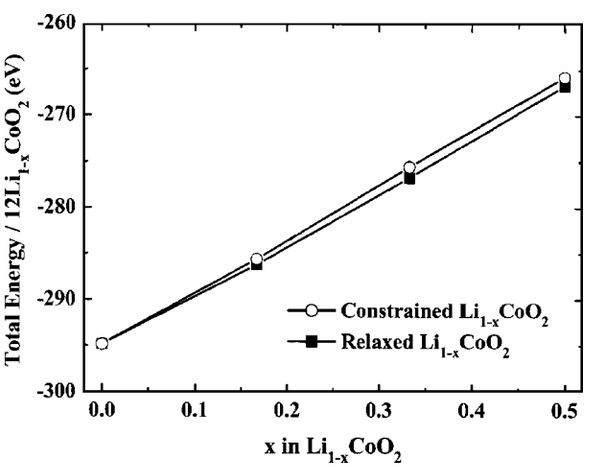

Figure 6. Total energies of $Li_{1-x}CoO_2$ are calculated with the constrained (at Li-ordered metastable state) and relaxed (at Li-ordered stable state) lattice. Four supercells of $x = 0$, 1/6, 1/3, and 1/2 in $Li_{1-x}CoO_2$ were used.

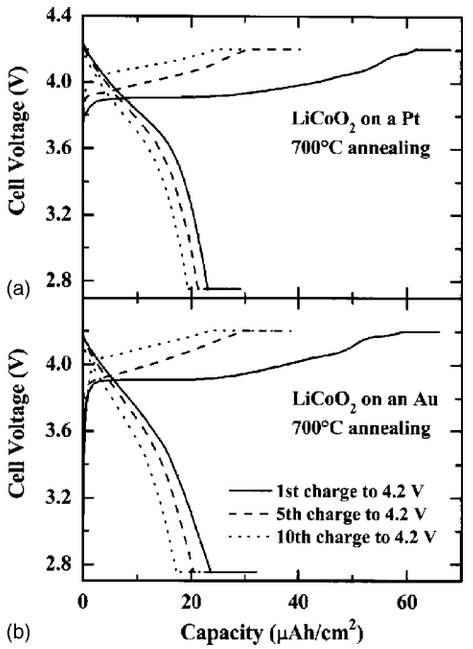

Figure 7. Voltage profiles of the $Li_{1-x}CoO_2$ thin films (a) on Pt and (b) on Au, for the XRD patterns at the 4.2 V charged state (Fig. 1 and 3). The cycling test was performed using a charge-cutoff voltage of 4.4 V at 400 $\mu A/cm^2$.

(c = 14.02 ± 0.06 Å), which may be due to the Li evaporation during deposition at 300°C.[28-30] When these cathode films were charged to 4.2 V during the first cycle, the lattice constant c increased to 14.32 ± 0.01 Å. In addition, diffraction-peak splitting is not observed, which is unlike the cathode films with a strong (003) texture (Fig. 1 and 3). The change of lattice constants, a and c, as a function of the cycle number (as shown in Fig. 9) is similar to that observed in the powder geometry.

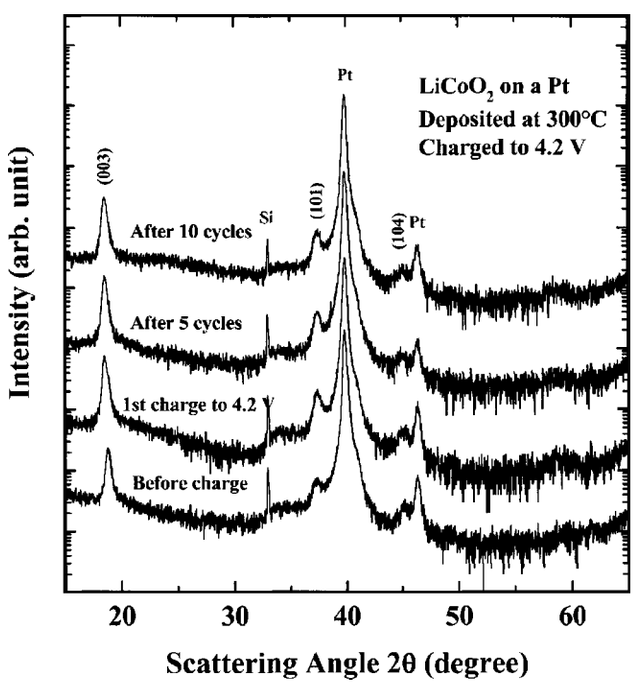

Figure 8. XRD patterns of $Li_{1-x}CoO_2$ thin films, before charge, after the 1st charge to 4.2 V and after five and ten cycles (between 4.4 and 2.75 V), then charged to 4.2 V. These cathode films were deposited at 300°C on a Pt/SiO_2 /Si substrate, without further annealing.

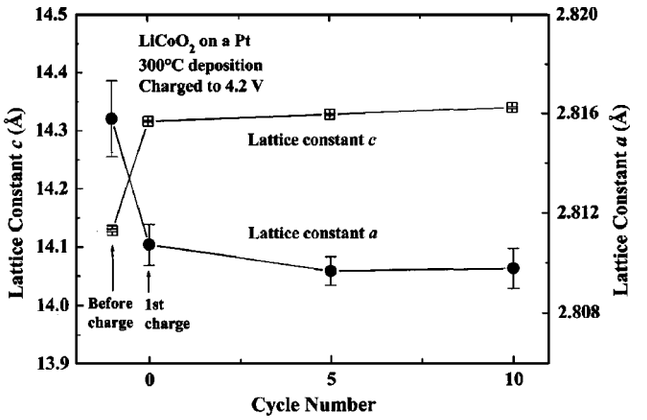

Figure 9. Changes in the lattice constant, a and c, as a function of cycle number for the $Li_{1-x}CoO_2$ thin films deposited at 300°C when charged to 4.2 V. The lattice constants were obtained from the XRD patterns shown in Fig. 8.

Conclusions

Thin-film $LiCoO_2$ cathodes were sputter-deposited under various deposition conditions, yielding distinct lattice-constant changes at the 4.2 V charged states. $LiCoO_2$ thin films with a strong (003) texture underwent limited lattice expansion during the first charge, which is unlike that observed for $LiCoO_2$ powders. The energy difference obtained by a pseudopotential total-energy calculation between the relaxed and constrained $Li_{0.5}CoO_2$ lattice was negligible, confirming no difficulty of limited lattice expansion. However, splitting of the (009) diffraction peak was observed at 4.2 V as cycling proceeded. In contrast, the lattice constants c of the $Li_{1-x}CoO_2$ thin films with a weak (003) texture expanded when first charged to 4.2 V. Further studies are clearly needed to correlate the thin-film microstructures and electrochemical properties.

Acknowledgments

This work was supported by the Center for Nanostructured Materials Technology under the 21C Frontier Programs of the Ministry of Science and Technology, by KOSEF through the Research Center for Energy Conversion and Storage at Seoul National University, and by Kumoh National Institute of Technology.

Seoul National University assisted in meeting the publication costs of this article.

References

1. J. N. Reimers and J. R. Dahn, *J. Electrochem. Soc.*, **139**, 2091 (1992).
2. T. Ohzuku and A. Ueda, *J. Electrochem. Soc.*, **141**, 2972 (1994).
3. H. Wang, Y.-I. Jang, B. Huang, D. R. Sadoway, and Y.-M. Chiang, *J. Electrochem. Soc.*, **146**, 473 (1999).
4. H. Wang, Y.-I. Jang, B. Huang, D. R. Sadoway, and Y.-M. Chiang, *J. Power Sources*, **81-82**, 594 (1999).
5. G. G. Amatucci, J. M. Tarascon, and L. C. Klein, *Solid State Ionics*, **83**, 167 (1996).
6. G. G. Amatucci, J. M. Tarascon, and L. C. Klein, *J. Electrochem. Soc.*, **143**, 1114 (1996).
7. C. Wolverton and A. Zunger, *Phys. Rev. B*, **57**, 2242 (1998).
8. M. K. Aydinol, A. F. Kohan, G. Ceder, K. Cho, and J. Joannopoulos, *Phys. Rev. B*, **56**, 1354 (1997).
9. H. Gabrisch, R. Yazami, and B. Fultz, *Electrochem. Solid-State Lett.*, **5**, A111 (2002).
10. Z. Chen and J. R. Dahn, *Electrochem. Solid-State Lett.*, **5**, A213 (2002).
11. Z. Chen and J. R. Dahn, *Electrochem. Solid-State Lett.*, **6**, A221 (2003).
12. J. Cho, Y. J. Kim, T.-J. Kim, and B. Park, *Angew. Chem., Int. Ed. Engl.*, **40**, 3367 (2001).
13. J. Cho, Y. J. Kim, and B. Park, *Chem. Mater.*, **12**, 3788 (2000).

14. J. Cho, Y. J. Kim, and B. Park, *J. Electrochem. Soc.*, **148**, A1110 (2001).
15. Y. J. Kim, T.-J. Kim, J. W. Shin, B. Park, and J. Cho, *J. Electrochem. Soc.*, **149**, A1337 (2002); Y. J. Kim, H. Kim, B. Kim, D. Ahn, J.-G. Lee, T.-J. Kim, D. Son, J. Cho, Y.-W. Kim, and B. Park, *Chem. Mater.*, **15**, 1505 (2003).
16. A. Van der Ven, M. K. Aydinol, and G. Ceder, *Phys. Rev. B*, **58**, 2975 (1998).
17. A. Van der Ven, M. K. Aydinol, and G. Ceder, *J. Electrochem. Soc.*, **145**, 2149 (1998).
18. C. Wolverton and A. Zunger, *Phys. Rev. Lett.*, **81**, 606 (1998).
19. D. Carlier, A. Van der Ven, C. Delmas, and G. Ceder, *Chem. Mater.*, **15**, 2651 (2003).
20. G. Ceder and A. Van der Ven, *Electrochim. Acta*, **45**, 131 (1999).
21. E. Deiss, A. Wokaum, J.-L. Barras, C. Daul, and P. Dufek, *J. Electrochem. Soc.*, **144**, 3877 (1997).
22. G. Kresse and J. Furthmuller, *Phys. Rev. B*, **54**, 11169 (1996).
23. G. Kresse and J. Furthmuller, *Comput. Mater. Sci.*, **6**, 15 (1996).
24. P. Hohenberg and W. Kohn, *Phys. Rev. A*, **136**, 864 (1964).
25. W. Kohn and L. Sham, *Phys. Rev. A*, **140**, 1133 (1965).
26. D. Vanderbilt, *Phys. Rev. B*, **41**, 7892 (1990).
27. H. J. Monkhorst and J. D. Pack, *Phys. Rev. B*, **13**, 5188 (1976).
28. P. J. Bouwman, B. A. Boukamp, H. J. M. Bouwmeester, H. J. Wondergem, and P. H. L. Notten, *J. Electrochem. Soc.*, **148**, A311 (2001).
29. J. B. Bates, N. J. Dudney, B. J. Neudecker, F. X. Hart, H. P. Jun, and S. A. Hackney, *J. Electrochem. Soc.*, **147**, 59 (2000).
30. Y.-I. Jang, N. J. Dudney, D. A. Blom, and L. F. Allard, *J. Electrochem. Soc.*, **149**, A1442 (2002).
31. P. J. Bouwman, B. A. Boukamp, H. J. M. Bouwmeester, and P. H. L. Notten, *J. Electrochem. Soc.*, **149**, A699 (2002).
32. Y. Iriyama, M. Inaba, T. Abe, and Z. Ogumi, *J. Power Sources*, **94**, 175 (2001).